Supporting information for

High Pyridine N-Doped Porous Carbon Derived from Metal-Organic Frameworks for Boosting Potassium-Ion Storage

Youpeng Li[a,b], Chenghao Yang[a,b*], Fenghua Zheng[a,b], Xing Ou[a,b], Qichang Pan[a,b], Yanzhen Liu[a,b], Gang Wang[a,b]

a *Guangzhou Key Laboratory for Surface Chemistry of Energy Materials, New Energy Research Institute, School of Environment and Energy, South China University of Technology, Guangzhou 510006, P. R. China*

b *Guangdong Engineering and Technology Research Center for Surface Chemistry of Energy Materials, New Energy Research Institute, School of Environment and Energy, South China University of Technology, Guangzhou 510006, PR China*

* Corresponding authors. *E-mail* addresses: esyangc@scut.edu.cn (C. Yang)

Supplementary Figures

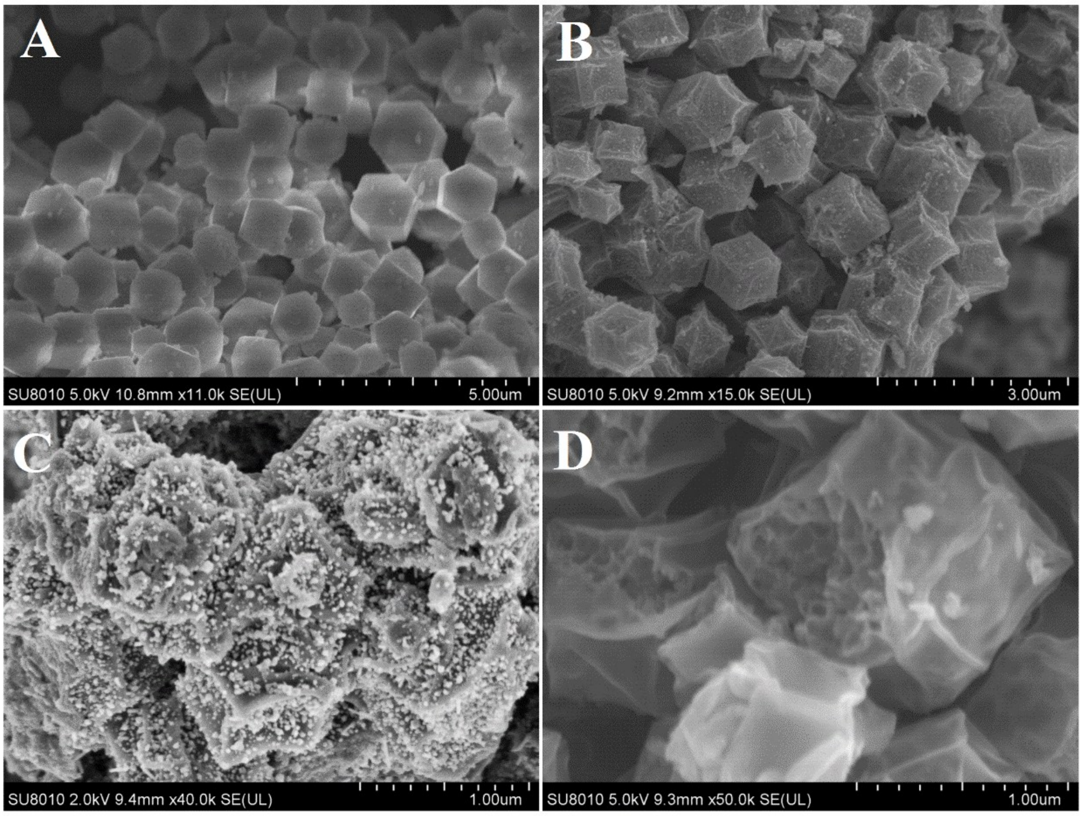

Figure S1 SEM images of ZIF-67 (A), CNPC-500 (B), CNPC-700 (C) and NCP-600 (D).

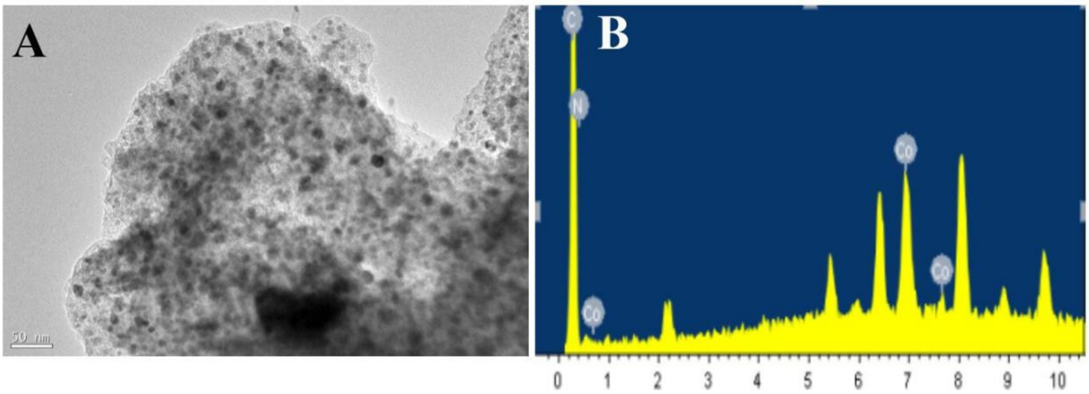

Figure S2 TEM image (A) and the corresponding EDS mapping (B) of CNPC-600.

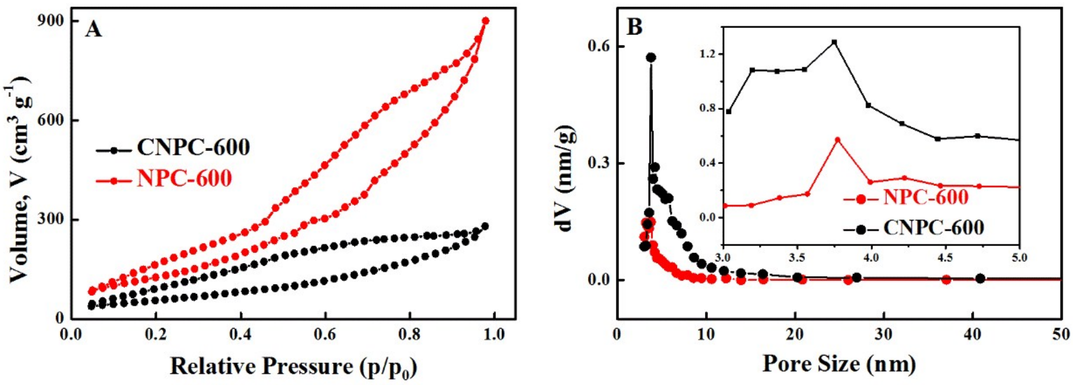

Figure S3 N_2 adsorption/desorption isotherms (A) and pore size distribution (B) of CNPC-600 and NPC-600, respectively.

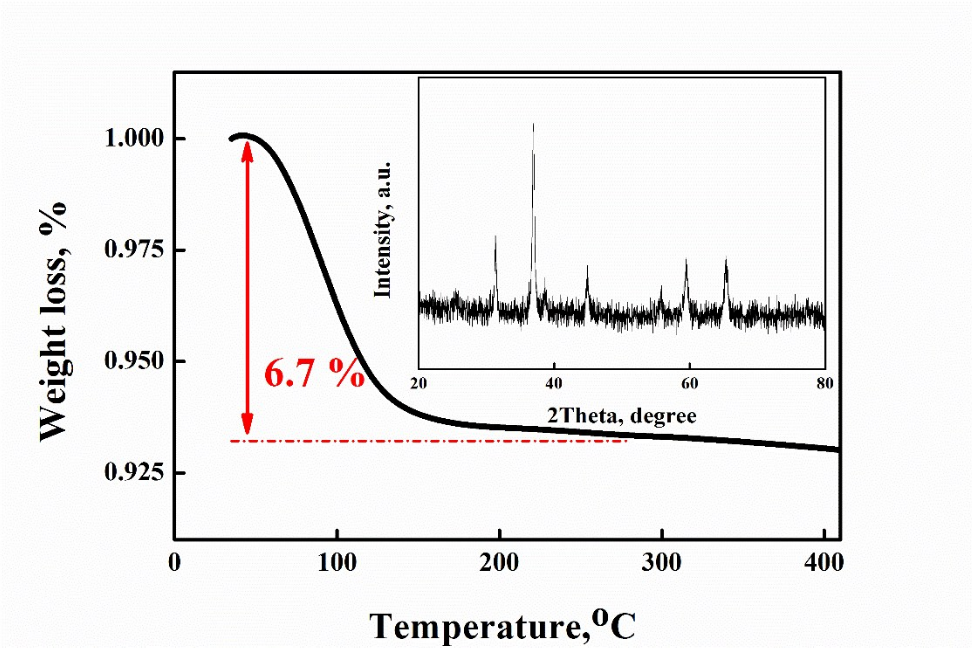

Figure S4 TGA curves of CNPC-600, the inset pattern is the XRD data of calcined sample.

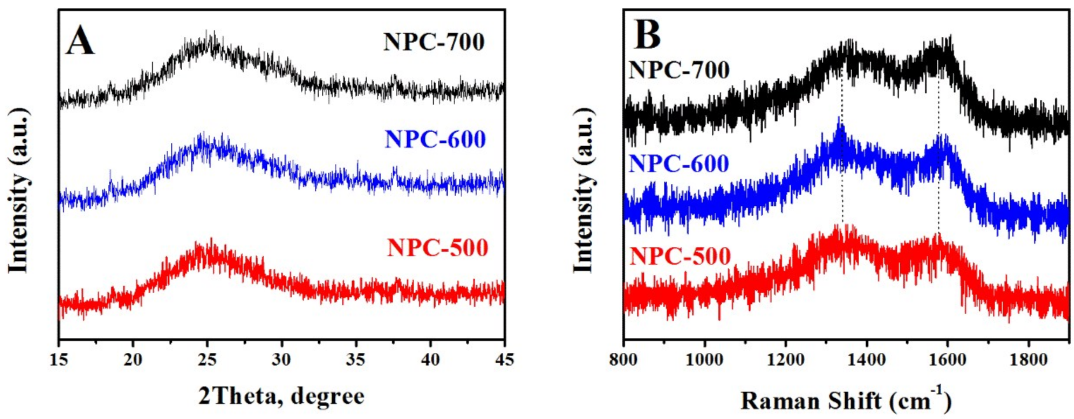

Figure S5 XRD patterns (A) and Raman spectra (B) of NPC-500, NPC-600 and NPC-700, respectively.

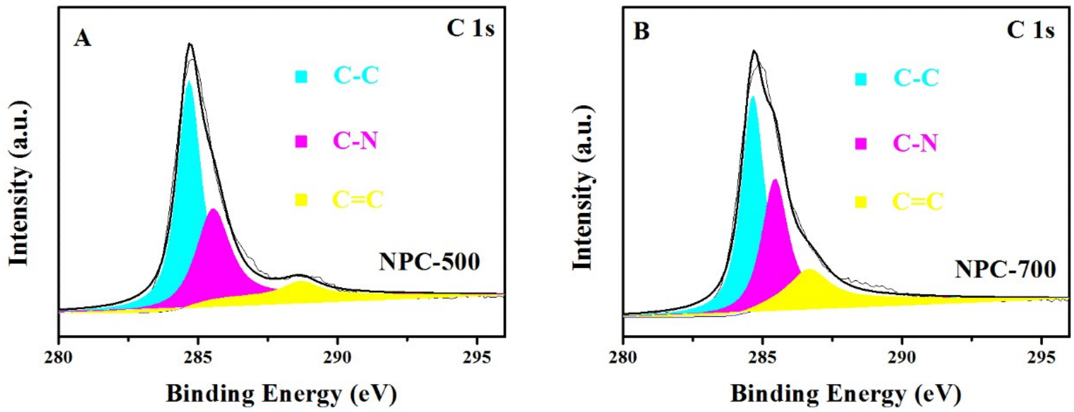

Figure S6 X-ray photoelectron spectroscopy (XPS) of C 1S for NPC-500 (A) and NPC-700 (B).

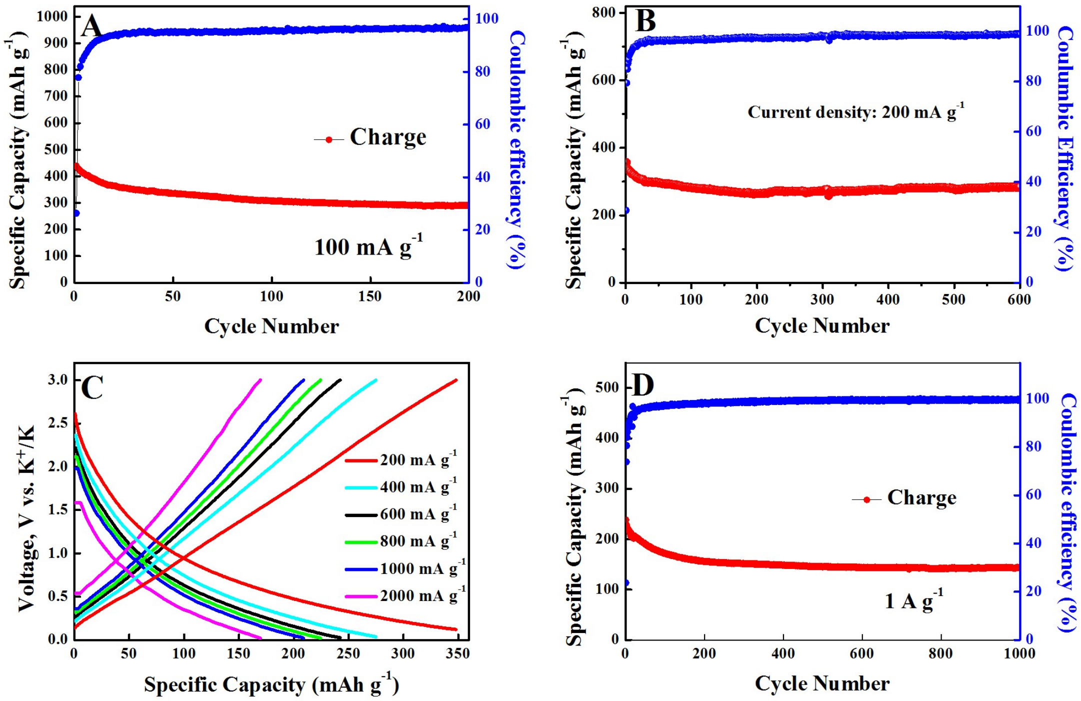

Figure S7 Cycle performance at 100 mA g^{-1} (A), 200 mA g^{-1} (B); galvanostatic charge/discharge curves at different rate (C) and cycle ability at 1 A g^{-1} (D) of NPC-600.

Table S1 Detailed Comparison of NPC-600 with other carbon-based anodes in PIBs.

Types of materials	Cycling performance		Rate performance		Ref (SI).
	Capacity(mAh g^{-1}) /cycles	Current rate (A g^{-1})	Capacity (mAh g^{-1})	Current (A g^{-1})	
Carbon nanofiber	170/1900	0.2	110	2	[S1]
Hard carbon microspheres	216/100	0.2	136	1	[S2]
Hard-Soft composite carbon	118/200	0.278	112	1	[S3]
Porous carbon paper	270/1200	0.02	156	2	[S4]
graphene	474/50	0.05	160	2	[S5]
N-doped carbon nanofibers	248/100	0.025	126	5	[S6]
Mesoporous carbon	197/200	0.2	144	1	[S7]
N-doped graphene	203/100	0.1	203	0.1	[S8]
N-rich hard carbon	205/200	0.03	154	0.3	[S9]
NPC-600	283.3/600	0.2	186.2	2	**This work**

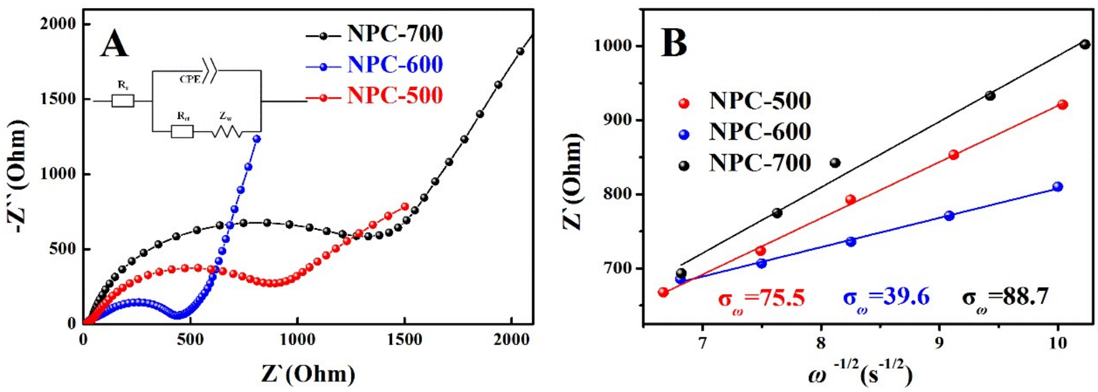

Figure S8 Electrochemical impedance spectroscopy (EIS) data of NPC-500, NPC-600 and NPC-700.

Table S2 The simulated results from electrochemical impedance spectra of NPC-500, NPC-600 and NPC-700 samples.

Sample	R_s (Ω)	R_{ct} (Ω)	D_{K^+} (cm^{-2} s^{-1})
NPC-500	13.45	783.47	9.54×10^{-14}
NPC-600	12.43	391.65	18.19×10^{-14}
NPC-700	21.57	1195.78	8.12×10^{-14}

The K ion diffusion coefficient (D_{K^+}) of NPC-500, NPC-600 and NPC-700 can be calculated according to the following equations:[S10]

$$D_{K^+} = \frac{R^2T^2}{2A^2n^4F^4C^2\sigma_w^2} \tag{1}$$

where R is the gas constant, T is the absolute temperature, A is the surface area of the cathode, n is the number of electrons per molecule during oxidization, F is the Faraday constant, C is the concentration of K^+ ion, σ_w is the Warburg factor which is relative with Z'.

$$Z' = R_s + R_{ct} + \sigma_w\omega^{-1/2} \tag{2}$$

R_s is the resistance of the electrolyte and electrode material, R_{ct} is the charge transfer resistance and ω is the angular frequency in the low frequency region.

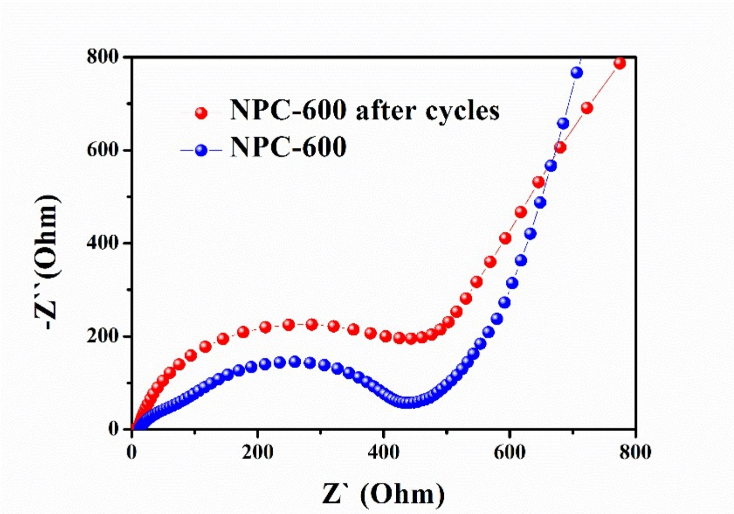

Figure S9 Electrochemical impedance spectroscopy (EIS) data of NPC-600 and NPC-600 after cycles.

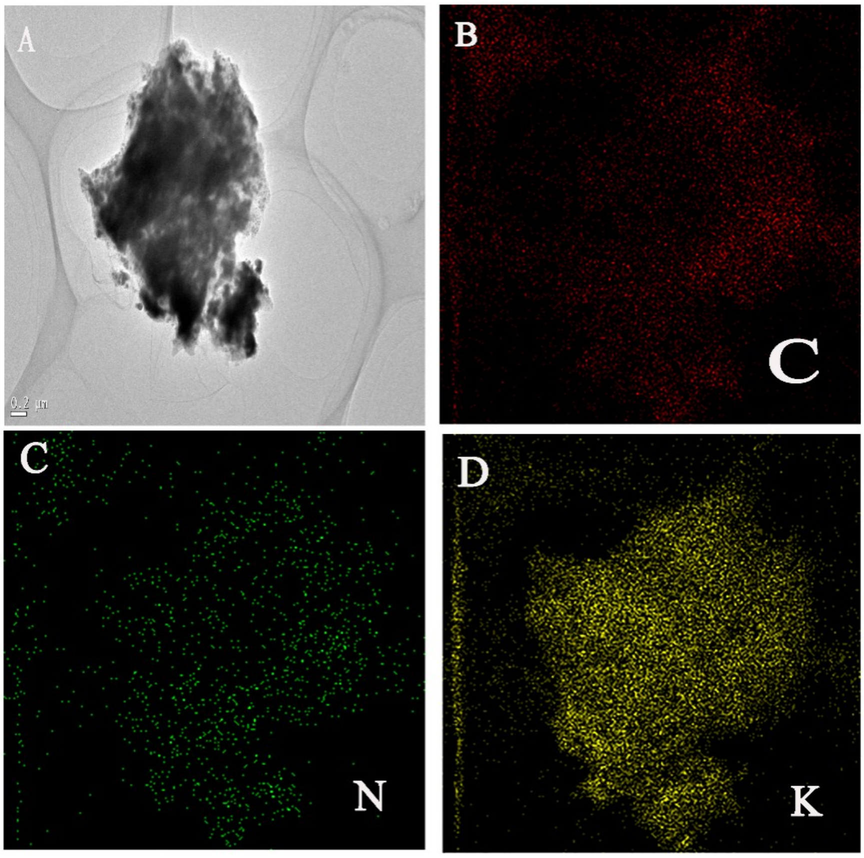

Figure S10 TEM image (A) and EDS mapping (B-D) at the fully potassiation state of NPC-600.

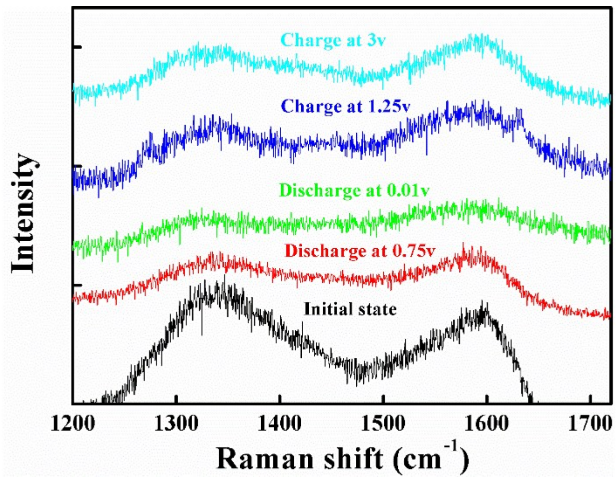

Figure S11 *Ex-situ* Raman spectra of NPC-600 at different charge/discharge states.

Table S3 The I_D/I_G values of NPC-600 at different charge-discharge states.

State	**I_D/I_G**
Initial state	1.02
Discharge at 0.75 V	0.98
Discharge at 0.01 V	0.91
charge at 1.25 V	0.96
charge at 3 V	0.99

Reference

[S1] R. A. Adams, J. M. Syu, Y. Zhao, C. T. Lo, A. Varma and V. G. Pol, *ACS Appl. Mater. Interfaces.*, 2017, **9,** 17872-17881.

[S2] Z. Jian, Z. Xing, C. Bommier, Z. Li and X. Ji, *Adv. Energy Mater.*, 2016, **6,** 1501874

[S3] Z. Jian, S. Hwang, Z. Li, A. S. Hernandez, X. Wang, Z. Xing, D. Su and X. Ji, *Adv. Funct. Mater.*, 2017, **27,** 1700324

[S4] M. Huang, K. Mi, J. Zhang, H. Liu, T. Yu, A. Yuan, Q. Kong and S. Xiong, *J. Mater. Chem. A.*, 2017, **5,** 266-274.

[S5] G. Ma, K. Huang, J.-S. Ma, Z. Ju, Z. Xing and Q.-c. Zhuang, *J. Mater. Chem. A.*, 2017, **5,** 7854-7861.

[S6] Y. Xu, C. Zhang, M. Zhou, Q. Fu, C. Zhao, M. Wu and Y. Lei, *Nat. commun.*, 2018, **9,** 1720.

[S7] W. Wang, J. Zhou, Z. Wang, L. Zhao, P. Li, Y. Yang, C. Yang, H. Huang and S. Guo, *Adv. Energy Mater.*, 2018, **8,** 1701648.

[S8] K. Share, A. P. Cohn, R. Carter, B. Rogers and C. L. Pint, *ACS Nano.*, 2016, **10,** 9738−9744.

[S9] C. Chen, Z. Wang, B. Zhang, L. Miao, J. Cai, L. Peng, Y. Huang, J. Jiang, Y. Huang, L. Zhang and J. Xie, *Energy Storage Mater.*, 2017, **8,** 161-168

[S10] N. Wu, W. Du, X. Gao, L. Zhao, G. Liu, X. Liu, H. Wu and Y. B. He, *Nanoscale.*, 2018, **10**, 11460-11466.